

# IDENTIFYING PATTERNS OF SATELLITE IMAGERY USING AN ARTIFICIAL NEURAL NETWORK

**Iskhaq Iskandar<sup>1,3</sup>, Azhar K. Affandi<sup>1</sup>, Dedi Setiabudidaya<sup>1</sup>, Muhammad Irfan<sup>1</sup>,  
Wijaya Mardiansyah<sup>1</sup>, and Fadli Syamsuddin<sup>2</sup>**

<sup>1</sup> Physics Department, Faculty of Matematic and Natural Sciences, Sriwijaya University, Palembang

<sup>2</sup> Agency for Assessment and Application Technology, Jakarta

<sup>3</sup> Environmental Research Center, University of Sriwijaya

e-mail: iskhaq@mipa.unsri.ac.id

**Abstract.** An artificial neural network analysis based on the self-organizing map (SOM) was used to examine patterns of satellite imagery. This study used  $3 \times 4$  SOM array to extract patterns of satellite-observed chlorophyll-*a* (chl-*a*) along the southern coast of the Lesser Sunda Islands from 1998 to 2006. The analyses indicated two characteristic spatial patterns, namely the northwest and the southeast monsoon patterns. The northwest monsoon pattern was characterized by a low chl-*a* concentration. In contrast, the southeast monsoon pattern was indicated by a high chl-*a* distributed along the southern coast of the Lesser Sunda Islands. Furthermore, this study demonstrated that the seasonal variations of those two patterns were related to the variations of winds and sea surface temperature (SST). The winds were predominantly southeasterly (northwesterly) during southeast (northwest) monsoon, driven offshore (onshore) Ekman transport and produced upwelling (downwelling) along the southern coasts of the Lesser Sunda Islands. Consequently, upwelling reduced SST and helped replenish the surface water nutrients, thus supporting high chl-*a* concentration. Finally, this study demonstrated that the SOM method was very useful for the identifications of patterns in various satellite imageries.

**Keywords:** *Downwelling, Monsoon, Self-organizing map, Satellite imagery, Upwelling*

## 1 INTRODUCTION

Variability of marine biology along the southern coast of Lesser Sunda Island was influenced by the seasonally varying monsoonal winds over the Indonesian region (Asanuma *et al.*, 2003). During the northwest monsoon (December-March), winds blow southeastward and drive onshore Ekman transport, which cause downwelling. On the other hand, during the southeast monsoon (June-October) the winds are predominantly southeasterly driving offshore Ekman transport. It usually starts in June, reaches its peaks in August, and diminishes in October/November (Susanto *et al.*, 2001; Qu *et al.*, 2005). This offshore Ekman transport is associated with upwelling of nutrient-rich subsurface-water supporting high primary productivity (Asanuma *et al.*, 2003; Susanto *et al.*, 2006).

Recently, modern satellite remote sensing provides frequent information that can be used to deduce the ocean processes. At the same time, however, these huge data sets often containing missing data and nonlinear terms are difficult to be analyzed. In particular, the satellite observation on ocean colour in the tropical ocean is uneven in time and space because useful data cannot be recorded through clouds. In this

study, we focus on the application of an artificial neural network for pattern recognition, so-called *self-organizing map* (SOM) (Kohonen, 2001). The ability of SOM to extract pattern from Sea-viewing Wide Field-of-view Sensor (SeaWiFS) satellite image is illustrated.

The SOM was first introduced for oceanographic data analysis in 1997 (Kropp and Klenke, 1997). They the SOM method to study the dynamical structures of tidal sediment in the German Wadden Sea. Since then, the SOM was widely used in oceanography community, in particular for satellite data analyses. In particular, Richardson *et al.* (2003) have demonstrated the useful of SOM for a construction of satellite imagery patterns, such as surface chlorophyll-*a* distribution. The SOM has also been used for pattern analysis of the oceanic current structures, both in the coastal area (Liu and Weisberg, 2005; 2007) and in the open sea (Iskandar *et al.*, 2008).

This study was designed to evaluate the useful of SOM method in constructing the pattern of satellite imageries. In particular, the study is intended to explore the seasonal pattern of surface chlorophyll-*a* distribution along the southern coast of the Lesser Sunda Islands.

## 2 DATA AND METHOD

### 2.1 Data

Monthly composites of the SeaWiFS chl-a concentration data over the nine-year period January 1998 – December 2006 were used in this study. The data were obtained using the GES-DISC interactive online visualization and analysis infrastructure (Giovanni) as part of the NASA's Goddard Earth Sciences (GES) Data and Information Services Center (DISC) available at <http://reason.gsfc.nasa.gov/Giovanni/>.

The SST used in this study was derived from the monthly Tropical Rainfall Measuring Mission (TRMM) Microwave Imager (TMI) data for period of January 1998 – December 2006. In addition, we used the monthly wind field data from QSCAT scatterometer for period of August 1997 – December 2006. Both SST and wind fields are available at <http://www.ssmi.com>.

### 2.2 Self-Organizing Map (SOM)

The SOM is one type of unsupervised Artificial Neural Network (ANN) that is mainly used for pattern recognition and classification (Kohonen, 2001). It performs a nonlinear projection from high-dimensional input data to a regular, low-dimensional array (usually two-dimensional unit). Each unit in the SOM array has a weight vector that is equal in dimension to the input samples. In practice, the SOM algorithm is outlined as follow:

#### a. Define shape and dimensions of SOM array

The shape of SOM array can be chosen to be either rectangular or hexagonal and its size is chosen by users. Note that the size of the output map depends on the level of details desired in the analysis. In this study, a  $3 \times 4$  SOM array was chosen after several trials.

#### b. Initialization step

After the shape and dimensions of the SOM array were chosen, the weight vectors were assigned with starting values, which can be chosen to be random values.

#### c. Training phase

The training process was started by sending the first input vector to the SOM array. Each node of the SOM array, then, was activated using an activation function. Here, we used the minimum Euclidian distance criterion. The node responding maximally to a given input vector (i.e. the smallest Euclidian distance) was selected to be the “winning” node,  $c_k$ :

$$c_k = \arg \min \|\bar{x}_k - \bar{w}_{ij}\| \quad (2-1)$$

where “arg” denotes index,  $\bar{x}_k$  indicates the present input vector and  $\bar{w}_{ij}$  is the weight vector. The “winning” node and its neighbouring nodes were trained by changing the weights in a manner so that they become closer to the input vector. The learning rule is defined as:

$$\bar{w}_{ij}(t+1) = \bar{w}_{ij}(t) + \alpha(t) \cdot \{\bar{x}(t) - \bar{w}_{ij}(t)\} \quad (2-2)$$

where  $\alpha(t)$  denotes the learning rate, which is specified by a linear time function:

$$\alpha(t) = \alpha_0(1 - t/T) \quad (2-3)$$

where  $\alpha_0$  is the initial learning rate and  $T$  signifies the length of training. Weight vectors of all neighbouring nodes will learn from the same input and their weights will be updated by a spatiotemporal decay function  $\varepsilon(t)$ . We have used a bubble function.

#### d. Convergence

The training process is repeated until convergence or until number of iteration is reached. The iteration process typically involves a large number of cycles ( $10^5 - 10^6$ ).

#### e. Classification

Once the iteration is over, the final SOM array can be used to classify the input data. In this study, we use the SOM toolbox (Kohonen et al., 1995) from the Helsinki University of Technology, which is available at [http://www.cis.hut.fi/research/som\\_lvq\\_pak.shtml](http://www.cis.hut.fi/research/som_lvq_pak.shtml).

## 3 RESULTS

Before performing SOM analysis to satellite image, some pre- and post-processing of the data is necessary. In this study, the chl-a data was transformed into a single row vector. Land and inner Indonesian sea regions were removed from the analysis (Figure 1). We decimated the 9 km resolution of SeaWiFS data into  $0.2^\circ \times 0.2^\circ$  resolution, so that the input data consists of 649 sea pixels. The final input matrix consists of 649 columns (pixels)  $\times$  108 rows (months).

The  $3 \times 4$  SOM array results are shown in Figure 2. Each particular node represents a typical structure within the input data, constructed from weights on that particular node. On the upper-two levels of the SOM array, we observed low concentration of chl-

a, whereas the lower-two levels of the SOM array are characterized by high concentration of chl-a. All SOM arrays exist in the input data (non zero frequencies) and the most common pattern was node (1,1) occurring in 37.9% of the images.

In order to demonstrate seasonal occurrence of each particular node in the SOM array, we constructed a hit-repartition map by calculating the number of months mapped to each node in the SOM array. Here, the hit-repartition map indicates the relative frequency of occurrence of each particular node in the SOM array (Figure 3).

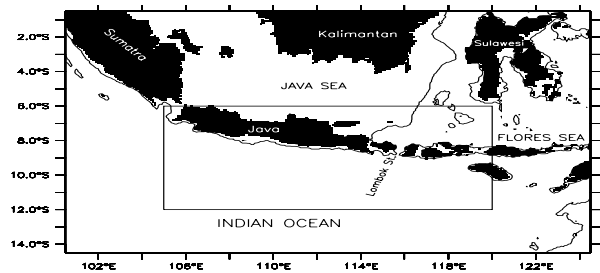


Figure 1. A map of the eastern tropical Indian Ocean. The study area is indicated by a square box covering a region between 105°E - 120°E and 12°S - 6°S. Contours indicate 100m isobaths

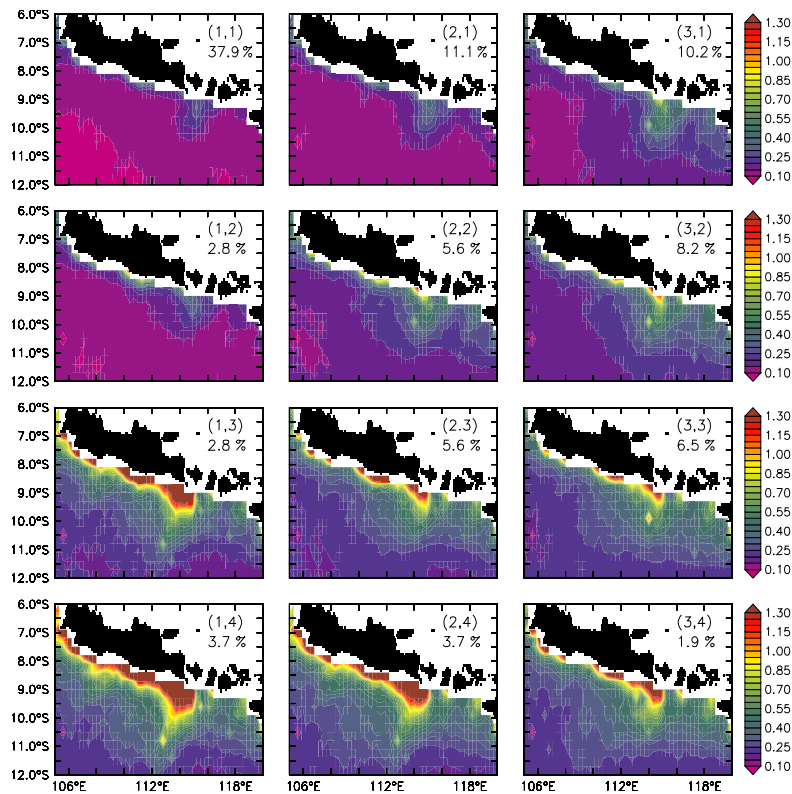


Figure 2. A 3 × 4 SOM array of 108 (January 1998 – December 2006) SeaWiFS images depicting surface chl-a concentrations along the Lesser Sunda Island. The notation of (1,1; 2,1;...; 3,4) indicates the matrix for SOM patterns. The percentile shows the occurrence frequency of the patterns in the total SOM patterns

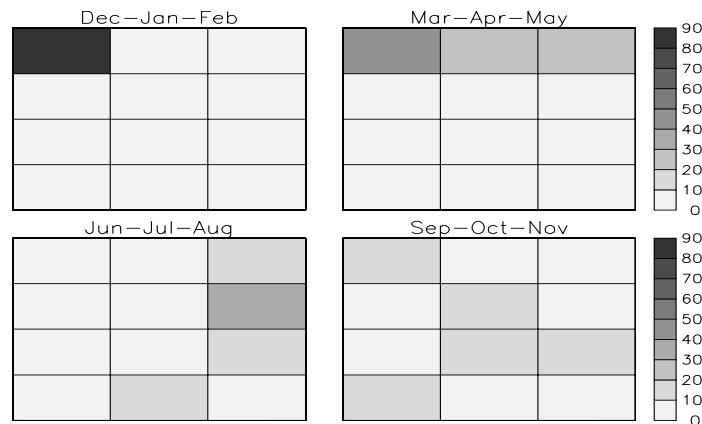


Figure 3. Seasonal frequency maps (%) of the 3 × 4 SOM array of SeaWiFS images, which correspond to the SOM pattern in Figure 2. The color indicates the frequency of occurrence of the pattern. The darkest color means the pattern is the most dominant pattern occurring in that season

It is shown that during southern summer (DJF), the node (1,1) dominates the variations of chl-a (>80%). This indicates that the concentration of chl-a during this season is very low (see Fig. 2). During southern fall (MAM), the hit-repartition map show more hits in the upper-most level of the SOM array, where node (1,1) still dominates the variation (~40%) and followed by nodes (2,1) and (3,1) occurring in ~20% of the images. The most frequent pattern (~30%) in the southern winter season (JJA) is node (3,2), which is characterized by high concentration of chl-a in the area around Lombok Strait. This season is also characterized by extremely high-concentration of chl-a indicated by node (2,4) which occurs in ~10% of the images. Moreover, nodes (3,1) and (3,3) also appear ~10% within the input data. In general, the southern winter season (JJA) is dominated by high concentration of chl-a. Finally, during southern spring (SON), the hit-repartition map is relatively distributed across the SOM array with maxima (~10%) at nodes (1,1), (2,2), (2,3) and (1,4).

The seasonal evolution of the chl-a patterns identified by the SOM can be interpreted in terms of upwelling and downwelling processes along the coast. In order to understand these dynamical processes, Figure 4 illustrates the seasonal

climatology of the winds superimposed on the sea surface temperature (SST) in this region.

It is shown that during southern summer (DJF), the winds are predominantly southeastward. These winds drive onshore Ekman pumping indicated by high SST in this region. During southern fall (MAM), the incoming downwelling Kelvin waves generated along the equatorial Indian Ocean reduced the upwelling process which driven by the local winds (Clarke and Liu, 1993; Sprintall et al., 2000; Iskandar et al., 2005). These incoming Kelvin waves induced high SST along the coast. On the other hand, during both southern winter (JJA) and spring (SON), strong northwestward winds drive offshore Ekman transport leading to reduce SST along the coast. This upwelling process helps replenish the surface water nutrients, thus supporting high chl-a concentration. It should be noted that during the southern spring season, the downwelling Kelvin waves are also excited along the equator and partly propagates southeastward as downwelling coastal Kelvin waves after reached the western coast of Sumatra. These Kelvin waves also induced warm SST from the equatorial region (Clarke and Liu, 1993; Sprintall et al., 2000; Iskandar et al., 2005).

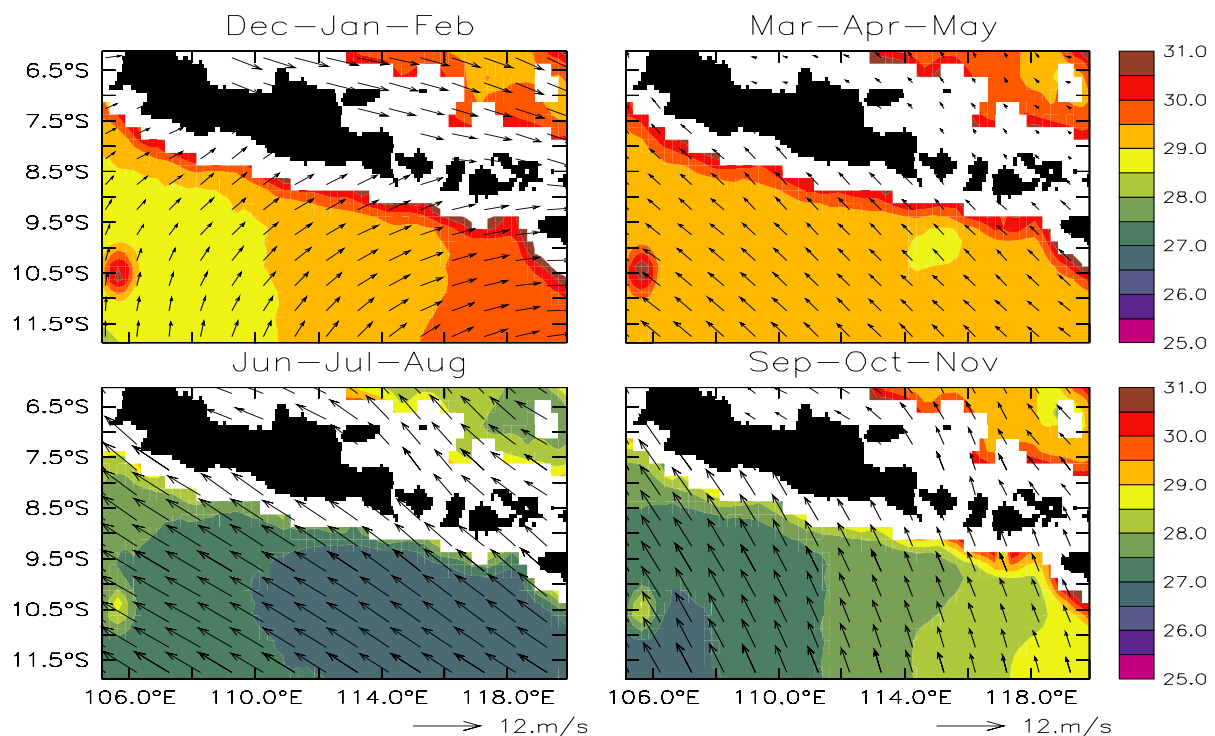


Figure 4. Seasonal climatology of surface winds (vector - m/s) superimposed on seas surface temperature (color - °C)

#### 4 CONCLUSIONS

We applied an artificial neural network (based on the SOM) analysis to examine characteristic patterns of the satellite-observed surface chl-a along the southern coast of the Lesser Sunda Islands. A  $3 \times 4$  SOM array is grouped into two composite categories: northwest and southeast monsoon patterns. The first pattern indicates low-concentration of chl-a, while the later is characterized by high-concentration of chl-a.

The synoptic variations of the surface chl-a are related to the variations of winds and SST. The southeast pattern is coincident with strong southeasterly winds and low SST. Offshore Ekman transport generated along the coast leads to upwelling of nutrient-rich water, which supports bloom of chl-a. On the other hand, the winds are predominantly southeastward during northwest pattern. These winds drive onshore Ekman transport leading to downwelling along the coast and increase SST.

This study demonstrates that the SOM is powerful tool for pattern recognition of large and complex satellite data sets. Note that the SOM algorithm is robust in handling missing data without priori estimation. One weakness of the SOM approach is that its size is defined by users, and this is arbitrary.

#### ACKNOWLEDGMENTS

We thank Dr. Tomoki Tozuka for useful discussion on the SOM technique. This study was supported by the Directorate General for Higher Education through International Collaboration and Publication Grant 2013 (No: 064/SP2H/PL/Dit.Litabmas/V/2013).

#### REFERENCES

- Asanuma, I., K. Matsumoto, H., Okano, T. Kawano, N. Hendiarti, and S. I. Sachoemar, 2003. *Spatial Distribution of Phytoplankton Along the Sunda Islands: The monsoon Anomaly in 1998*, J. Geophys. Res., 108(C6), 3202, doi: 10.1029/1999JC000139.
- Clarke, A. J. and X. Liu, 1993. *Observations and Dynamics of Semiannual Sea Levels Near the Eastern Equatorial Indian Ocean Boundary*, J. Phys. Oceanogr., 23, 386-399.
- Iskandar, I., W. Mardiansyah, Y. Masumoto and T. Yamagata, 2005. *Intraseasonal Kelvin Waves Along the Southern Coast of Sumatera and Java*, J. Geophys. Res., 110, C04013, doi:10.1029/2004JC002508.
- Kohonen, T., 2001. *Self-Organizing Maps*, 3<sup>rd</sup> ed., 501pp., Springer-Verlag Berlin Heidelberg, New York.
- Kropp, J. and T. Klenke, 1997. *Phenomenological Pattern Recognition in the Dynamical Structures of Tidal Sediments from the German Wadden Sea*, Ecological Modelling, Vol. 103, No. 2-3, 151-170, ISSN 0304-3800.
- Liu, Y. and R. H. Weisberg, 2005. *Patterns of Ocean Current Variability on the West Florida Shelf using the Self-Organizing map*, Journal of Geophysical Research, Vol. 110, C06003, doi: 10.1029/2004JC002786, ISSN 0148-0227.
- Liu, Y. and R. H. Weisberg, 2007. *Ocean Currents and Sea Surface Heights Estimated Across the West Florida Shelf*, Journal of Physical Oceanography, Vol. 37, 1697-1713, ISSN 0022-3670.
- Qu, T., Y. Du, J. Strachan, G. Meyers, and J. Slingo, 2005. *Sea Surface Temperature and its Variability in the Indonesian Region*, Oceanography, 18, 50-61.
- Richardson, A. J., C. Risien, and F.A. Shillington, 2003. *Using Self-Organizing Maps to Identify Patterns in Satellite Imagery*, Progress in Oceanography, Vol. 59, No. 2-3, 223-239, ISSN 0079-6611.
- Sprintall, J., A. L. Gordon, R. Murtugudde and R. D. Susanto, 2000. *A Semiannual Indian Ocean Forced Kelvin Wave Observed in the Indonesian Seas in May 1997*, J. Geophys. Res., 105, 17,217 – 17,230.
- Susanto, R.D., A.L. Gordon, and Q. Zheng, 2001. *Upwelling Along the Coasts of Java and Sumatera and its Relation to ENSO*, Geophys. Res. Lett., 28, 1599-1602.
- Susanto, R.D., T.S. Moore II, and J. Marra, 2006. *Ocean Color Variability in the Indonesia Seas During the SeaWiFS era*, Geochem, Geophys., Geosys., 7, doi: 10.1029/2005GC001009.

